Photonic crystal waveguides and their applications

Invited Paper

Yidong Huang (黄翊东), Xiaoyu Mao (毛晓宇), Chao Zhang (张 超), Lei Cao (曹 磊), Kaiyu Cui (崔开宇), Wei Zhang (张 巍), and Jiangde Peng (彭江得)

State Key Laboratory of Integrated Optoelectronics, Department of Electronic Engineering, Tsinghua University, Beijing 100084

Received June 10, 2008

Two-dimensional (2D) slab photonic crystal waveguides (PCWGs) on silicon-on-insulator (SOI) wafer were designed and fabricated. Full photonic band gap, band gap guided mode, and index guided mode were observed by measuring the transmission spectra. Mini-stop-bands in the PCWG were simulated with different structure parameters. Coupling characteristics of PCWG were investigated theoretically considering the imperfections during the fabrication process. It was found that suppressing power reservation effect can realize both short coupling length and high coupling efficiency.

OCIS codes: 160.5298, 230.7370.
doi: 10.3788/COL20080610.0704.

Photonic crystal (PC) has been focused on since it was proposed by Yablonovitch[1] and John[2] in 1987, as it can provide a novel way to guide, control, and manipulate the photons. In various PC structures, two-dimensional (2D) PC slabs, which are normally made by periodically patterning an array of air holes in high refractive index materials slabs, have received considerable attention in recent years[3−6] for its in-plane band-gap and compatible fabrication method with the traditional semiconductor wafer process. Inducing a line defect to the slab, PC would form a band gap confinement PC waveguide (PCWG)[7], which is the fundamental part of most PC based devices[8].

This paper reviews our present research work on the PCWG. A 2D slab PCWG on silicon-on-insulator (SOI) wafer was designed and fabricated with traditional stripe waveguides for joint. By measuring the transmission spectra, full photonic band gap, band gap guided mode, and index guided mode were observed near 1.55 μm. Mini-stop-bands in the PCWG were discussed with different structure parameters. It is found that their centre frequency is very sensitive to the refractive index of the substance filled in the holes of PC. Coupling characteristics of PCWG were investigated theoretically by considering the imperfections during the fabrication process. It was found that suppressing power reservation effect can realize both short coupling length and high coupling efficiency.

Figure 1(a) shows the simulation model of the PCWG. The refractive index of the background and the substance filled in the holes is n_2 and n_1, respectively. The lattice constant is a, the radius of the air holes is r, and r/a is taken as a key structure factor for the following discussions because it decides the air-filling factor of the PCs $f \propto (r/a)^2$. We designed the PCWG by plane wave expansion method and finite-difference time-domain (FDTD) simulation to ensure the band gap guided mode around the wavelength of 1.5 μm. Here, size enlarge was considered because hole size would be enlarged during the fabrication. Line defect PCWGs along Γ-K direction were fabricated. Figure 1(b) shows the structure. SOI wafer with a 200-nm-thick silicon film on the top and a 3000-nm-thick buried SiO_2 layer was used. Using a ZEP-520A resist mask, PC pattern was generated perfectly by electron beam (EB) lithography. Then an inductively coupled plasma (ICP) dry etching was employed to transfer the pattern to the silicon film. After removing the resist mask, a 600-nm-thick SiO_2 cover layer was deposited on the surface to form a symmetry SiO_2 clad structure for reducing the radiation loss in the vertical direction. Finally, we ground the wafer to about 100-μm thick, and cleaved them into about 1 mm-long samples for measurement. We removed some sample's upper SiO_2 cover layer by HF etching to verify the size and shape of the holes by scan electron microscope (SEM). Figure 2 are the SEM pictures for a slab PC without line defect and a line defect PCWG along Γ-K direction. The period a and the radius r of the PC are 380 nm and 90 nm, respectively. The coupling loss between a tapered fiber and a stripe waveguide was measured. For tapered fiber with 1.7-μm focus diameter, we found that a 2-μm wide waveguide had the lowest coupling loss of −7 dB per facet. Therefore 2-μm-wide waveguide was used for

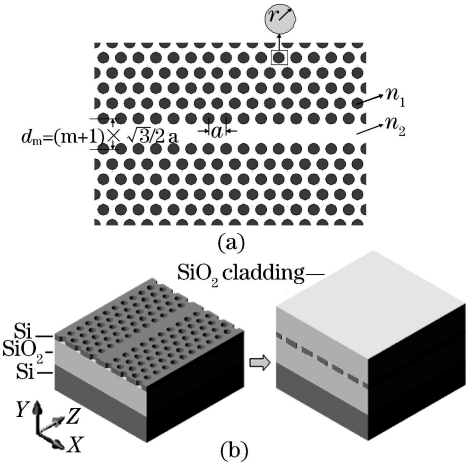

Fig. 1. (a) Simulation model and (b) symmetry SiO_2 clad structure.

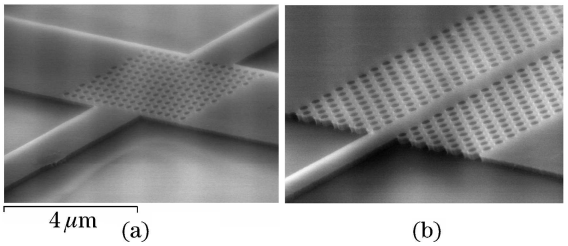

Fig. 2. SEM pictures of the fabricated 2D slab (a) PC and (b) PCWG.

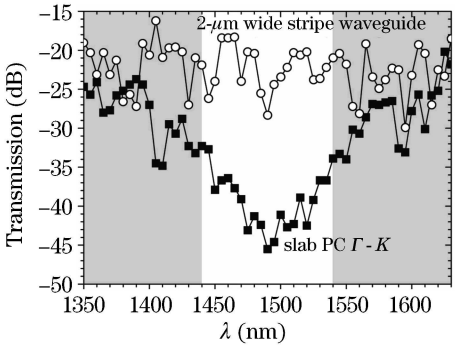

Fig. 3. Transmission spectra of the slab PC (square marks) and stripe waveguide without PC structure (circle marks).

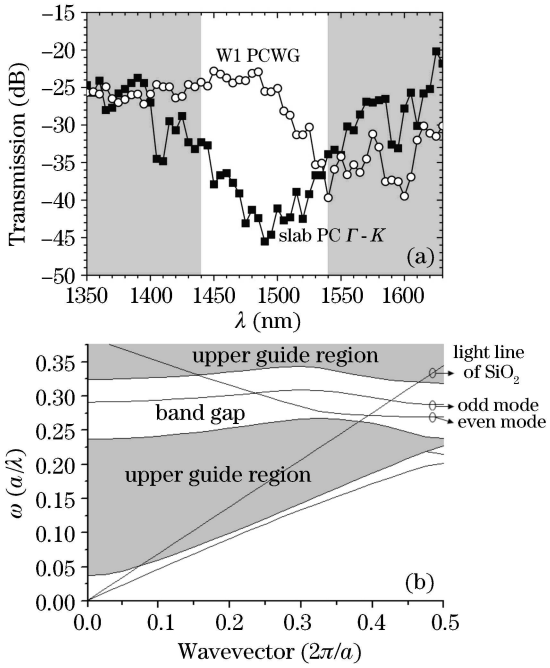

Fig. 4. Transmission spectra of the slab PC (square marks) and W_1 PCWG (circle marks).

the PC to couple the light in and out, while for PCWG, we added a 100-μm-long tapered waveguide to reduce the coupling loss to the narrow line defect.

The transmission spectra were measured. The measurement system was composed of a tunable laser with tuning range from 1350 to 1630 nm, a fiber polarization controller, a precise fiber alignment system with computer controlling, and an optical power meter. The polarization state was determined by using a polarization controller.

Figure 3 shows the transmission spectra of the slab PC with 2-μm-wide joint stripe waveguides to let the light input along Γ-K direction, compared with that measured from the same joint waveguide without the slab PC structure. It can be seen that, even though there are only 10 periods of holes in the light propagation direction, a deep transmission dip still formed due to the strong index comparison between Si and SiO_2. The blank region among the shadow areas is the photonic band gap calculated using the practical structure parameters measured by SEM. The measured transmission dip is in good agreement with the calculated band gap.

We used the same PC structure (a = 380 nm, r = 90 nm) to form a W_1 PCWG (its width is 1.73a), which has a single line of missing holes and the length of 60 periods. Its transmission spectra are shown in Fig. 4(a) by circle marks. We can see that, comparing with the transmission spectra of the slab PC, light can propagate in the band gap region. This corresponds with the line defect mode, namely band gap guided mode. We calculated the dispersion curve of the measured W_1 PCWG by 2D effect refection index-plane wave expansion methods. Figure 4(b) shows the results. It can be seen that there are two guided modes in the band gap. One is even mode, its majority electrical field component E_x is even symmetry to the y-z plane and the other is odd mode with odd symmetry. Because the odd mode cannot be excited easily, we can only consider single even defect mode in the band gap. The calculation results show that, the even defect mode extends off the band gap into the upper guide region. This phenomenon was confirmed from the experimental results in Fig. 4(a), where the power of the defect mode did not reduced obviously at the short wavelength edge. From the simulation results, we know that the defect mode is above the light line in most wavelength region. Because of the short propagation distance, the loss is not too much. We compared transmission spectrum of W_1 PCWG with different lengthes and found that 120-period-length PCWG suffers more loss above light line than the 60-period ones. There are some ripples in our measured transmission spectra. This phenomenon was also reported in Ref. [7]. It can be considered as the Fabry-Perot (F-P) oscillation caused by reflection of the sample's facet or the interface between the PCWG and joint stripe waveguides. Imperfection of the EB lithography, which induces some microcavity-like effects, and instability of the measurement system, also can cause such ripples.

Mode-coupling between the defect modes in PCWGs could result in mini band gaps (mini stop bands: MSBs) in the frequency region of the defect modes and cute dips in their transmission spectrum. Researches have revealed that MSB appears when the mode coupling occurs between two modes satisfying the following three factors: these two modes propagating in anti-direction; the wave vectors of them differed by an integer number of reciprocal lattice vectors; and they have the same symmetry[9].

As shown in Fig. 1(a), the width of the PCWG, denoted as d_m, can be expressed as $d_m = (m+1)(\sqrt{3}/2)a$, and the waveguide is denoted as W_m. Here, m can be a fraction with continuously varied d_m when adjusting the location of the two rows holes beside the waveguide. For instance, for W_1 waveguide, the width d_1 is 1.73a, and $W_{1.75}$ waveguide corresponds to the width of $d_{1.75}$ = 2.38a.

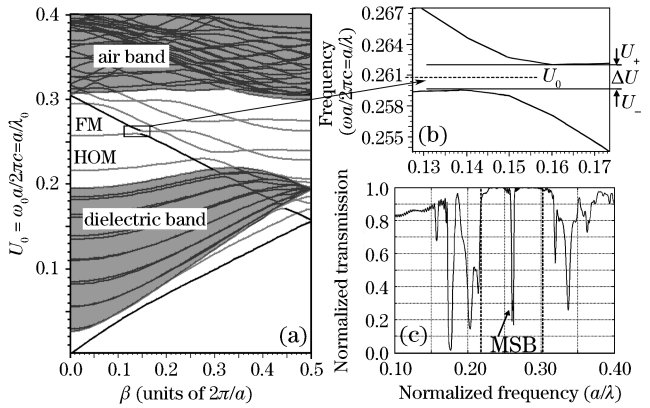

Fig. 5. MSB phenomenon in 2D PCWG. (a) Dispersion relation of a W_3 waveguide with $r/a = 0.32$, $n_1 = 1$, and $n_2 = 3.3$; (b) center frequency and bandwidth of MSB; (c) transmission spectrum of the W_3 PCWG and the dip corresponding to the MSB.

Figure 5(a) are the calculation results for a W_3 PCWG with $n_1 = 1.0$, $n_2 = 3.3$, and $r/a = 0.32$. There is a photonic band gap for TE polarization between the air band and dielectric band, covering the normalized frequency range of u from 0.22 to 0.3 ($u = a/\lambda$). Within the band gap, there are several guided modes (defect modes). The fundamental mode (FM) signed by the dashed line couples with one of the high-order modes (HOMs) and generates the corresponding MSB. Detail of the MSB is shown in Fig. 5(b), where the center frequency and bandwidth of MSB are defined as U_0 and ΔU, respectively. The transmission spectrum of this PCWG was calculated by FDTD method and shown in Fig. 5(c). It can be seen that the central frequency of the dip corresponds to the central frequency of the MSB in the dispersion relation.

We studied the properties of MSB in PCWG. It was found that MSBs can only exist in PCWGs with adequate width and air-filling factor. Namely, for certain air-filling factor, there is no MSB until the width of PCWG is large enough. We defined the narrowest width for generating MSBs as the critical width. Figure 6 shows the critical width as a function of air-filling factor r/a, where $n_1 = 1.0$ and $n_2 = 3.3$. MSBs exist in the gray area above the critical line. It can be seen that the critical width decrease linearly with the increase of r/a. The reason can be known as follows. When air-filling factor of PCWGs increase, the air-band of PCs moves to higher frequency, and results in the broadening of band-gap of

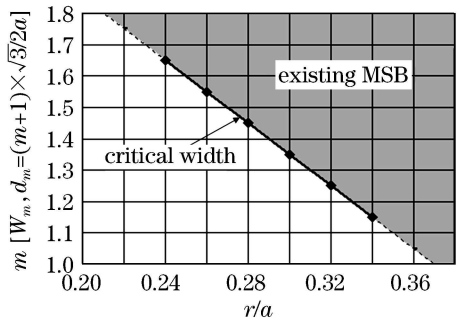

Fig. 6. Critical width of PCWGs for generating MSBs. The gray area represents the MSBs appearing area of waveguides when $n_1 = 1.0$, $n_2 = 3.3$.

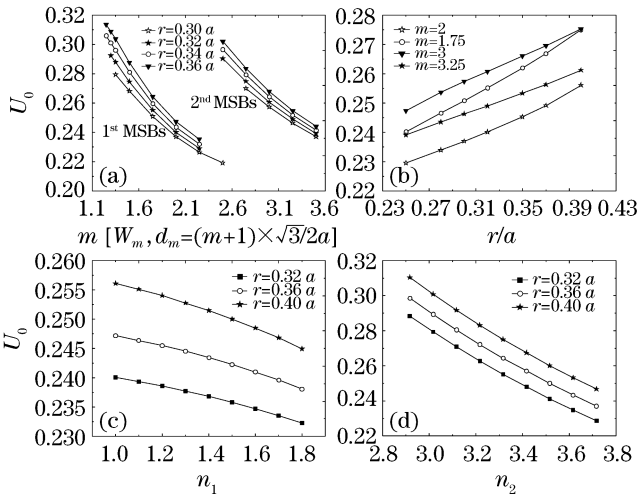

Fig. 7. Structure parameter dependences of the central frequency U_0 of MSBs.

PC. Therefore, the guiding modes located in the gap increases, which let the coupling between FM and HOM occurs easily and MSB appears even with narrow waveguide width.

The central frequency and the bandwidth are strongly depends on the structure parameters, such as d_m, r/a, n_1, and n_2. Figure 7(a) shows the simulation results for the dependence of central frequency U_0 on d_m with fixed $n_1 = 1.0$, $n_2 = 3.3$, and different r/a. It can be seen that, with certain air-filling factor, when the waveguide width broadens, the MSBs would move toward lower frequency, until out of the band-gap of PC. At the same time, another HOM satisfying coupling conditions would move down into the gap from the top of band-gap, and then it will couple with FM to generate another new MSB. Therefore, the lines in Fig. 7(a) are ruptured into two groups, which are corresponding to two kinds of MSBs when FM couples with two different HOMs. Figure 7(b) shows the dependence of U_0 on r/a. For PCWGs with certain width, the central frequency of MSBs increases with the air-filling factor. This can be interpreted just like the illustration for Fig. 6. Simulation results in Figs. 7(c) and (d) correspond to waveguide W_2 and $W_{1.75}$, respectively. It is revealed that the central frequency of MSBs decreases linearly with the increasing of either n_1 or n_2. The reason lies in the fact that with the increasing of dielectric refractive index n_1 or n_2, the air band or dielectric band shown in Fig. 5 will move down, and the MSBs, as well as their central frequency, also shift toward lower frequency. The relation between U_0 and n_1 means that MSBs are quite sensitive to the dielectric substance in the holes of PC structure. Therefore the dip on the transmission spectrum will shift with the varieties of n_1. Figure 8 shows the calculation results for W_2 waveguide with fixed $n_2 = 3.32$ and $r/a = 0.36$, where n_1 varies from 1.0 to 1.8. It is obvious that the transmission dip corresponding to MSB experiences red shift as n_1 increases. These results give us a hint that MSB effect can be used to develop a refractive index sensor for fluid analyze.

The fact that bandwidth of MSBs ΔU is related to coupling constant and group velocity index of the two coupling modes has been studied and reported in Ref. [10].

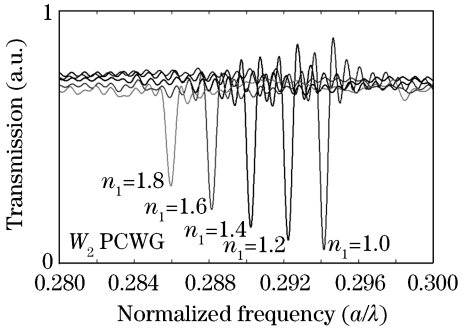

Fig. 8. Cute dip shifts with the varieties of n_1 from 1.0 to 1.8 for W_2 PCWG.

All structure parameters influence the dispersion relations and the defect modes of PCWGs, so the modes coupling, as well as ΔU, would vary with the change of structure parameters. Calculation results show that the width of PCWGs influences ΔU dramatically while the effect of dielectric refractive indices is faint, and the air-filling factor almost doesn't influence ΔU at all.

Optical coupler is one of the basic building blocks in photonic integrated circuits. Compared with conventional optical coupler, PCWG optical coupler has shorter coupling length and more adjustable properties. The coupling characteristics of PCWGs, such as coupling frequency, coupling length, coupling efficiency (ratio of the input power of the coupling waveguide to the total output power), total power transferring through couplers, etc., are sensitive to the structure of PCWG optical coupler, namely the length and width of the waveguide, the radii of air holes at the coupling region, and the ratio of the radii of air holes to the lattice constant, etc. This implies the possibility to obtain ideal coupling properties by adjusting these structure parameters properly.

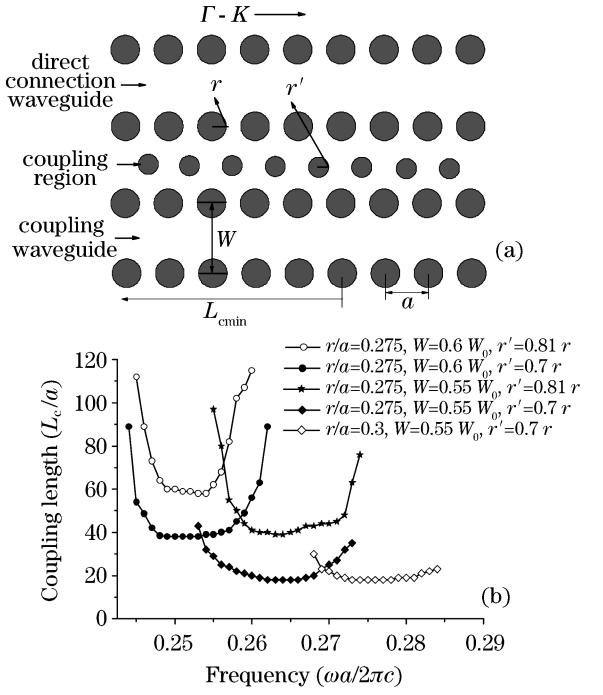

Fig. 9. (a) Simulation model for PC coupler; (b) different normalized coupling lengths and coupling frequencies of PC couplers of different structures versus normalized frequency.

Coupling length of photonic crystal directional coupler (PCDC) was analyzed with changed structure parameters using the finite-difference time-domain (FDTD) method. Figure 9(a) shows the simulation model. The radii of air holes in the middle row between two single line defect waveguides (coupling region), a very important parameter to affect coupling properties, is indicated by r'. Figure 9(b) shows the different normalized coupling length of PC coupler with different structure versus normalized frequency. Comparing lines a and b or c and d, where r/a and W are the same and only r' is changed from $0.81r$ to $0.7r$, it can be found that smaller r' correspond to shorter coupling length in all the frequency region. Lines a and c or b and d, where only W is changed from $0.6W_0$ to $0.55W_0$ with fixed r' and r/a, show narrower waveguides have both shorter coupling length and higher coupling frequency. Line e has almost the same coupling length and higher coupling frequency compared with line d.

From simulation, we found mode power reservation at the coupling region of the PC coupler, as shown in Fig. 10(a). This could reduce their coupling efficiency, especially in the case that we do the efforts to shorten the coupling length by reducing the width of PCWG or decreasing the radii of air holes at the coupling region. A kind of improved structure for PCWG couplers by simply increasing the radii of air holes at the post coupling region was proposed. The simulation results demonstrated that the coupling efficiency can be enhanced dramatically by suppressing the effect of mode power reservation, and therefore both short coupling length (about $20a$) and high coupling efficiency (about 90%) can be obtained[11].

In fact, there are always some imperfections during the fabrication process which results in some deviation from the ideal PC structure. We consider the air hole size nonuniformity as a normal distribution in which the air hole radii follow a normal "bell curve" distribution with a standard deviation σ_1, while the standard deviation of the position misalignment along and perpendicular

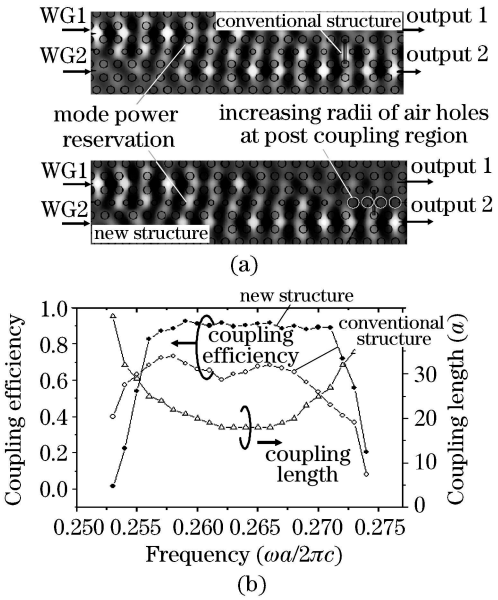

Fig. 10. (a) New structure can suppress the effect of mode power reservation; (b) coupling efficiency can be improved in the new structure with a short coupling length.

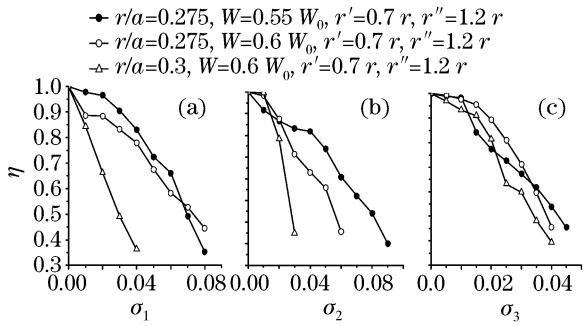

Fig. 11. Simulation results for deterioration of transmission efficiency of PC coupler due to σ_1, σ_2, σ_3.

to the waveguide direction are indicated by σ_2 and σ_3, respectively. The deterioration of transmission efficiency of PC coupler due to σ_1, σ_2, and σ_3 was simulated by FDTD method with different r/a and waveguide width W. Here we defined the ratio of output power of actual PC coupler P_{20} to that of ideal PC coupler P_2 as η for analyzing the influences of σ_1, σ_2, and σ_3. For PC coupler with different r/a and W, the waveguide length was selected to be the minimum coupling length. The results are shown in Fig. 11. It can be found that for the PC couplers with the same structure parameters, σ_3 has a more powerful influence on their performances than σ_1 and σ_2. That is, the behavior of PC coupler is more sensitive to the accuracy of air hole position perpendicular to the waveguide direction. Meanwhile, we can see that a small r/a is helpful to improve the robustness of PC coupler. When $r/a = 0.275$ and $W = 0.55W_0$, if we need $\eta = 0.8$, σ_1, σ_2, and σ_3 should be controlled within 0.04, 0.04 and 0.015, respectively.

This paper reported the research results on the PCWG. A 2D slab PC and a line defect PCWG based SOI structure were designed and fabricated. Transmission spectra of them were measured and analyzed. Full photonic band gap around the wavelength of 1.5 μm was obtained from the 2D slab PC and the defect mode within the band gap was observed for the line defect PCWG. We have investigated the structure parameters dependence of MSBs in PCWGs. The simulation results reveal that MSBs only appear in PCWGs with adequate width. The relations between the central frequency of MSBs and various structure parameters of PCWGs have been studied. It is found that the central frequency of MSBs is sensitive to the substance filled in the holes, which makes it possible to develop integrative fluid sensor. We also studied the influences of structure parameters and fabrication imperfections on the behavior of PC coupler theoretically. An improved structure of PC coupler was proposed by simply increasing the radii of air holes in the post coupling region to enhance the coupling efficiency by suppressing the effect of mode power reservation. As for the influence of fabrication imperfections, research results show that air hole position perpendicular to the waveguide direction has a most powerful influence on PC coupler and reducing filling factor is helpful to improve the robustness of PC coupler.

This work was supported by the National Natural Science Foundation of China (NSFC-60537010), and the National "973" Program of China (No. 2007CB307004 and 2006CB302804). Y. Huang's e-mail address is yidonghuang@tsinghua.edu.cn.

References

1. E. Yablonovitch, Phys. Rev. Lett. **58,** 2059 (1987).
2. S. John, Phys. Rev. Lett. **58,** 2486 (1987).
3. M. Loncar, D. Nedeljkovic, T. Doll, J. Vuckovic, and A. Schever, Appl. Phys. Lett. **77,** 1937 (2000).
4. E. Chow, S. Y. Lin, J. R. Wendt, S. G. Johnson, and J. D. Joannopoulos, Opt. Lett. **26,** 286 (2001).
5. Y. Sugimoto, Y. Tanaka, N. Ikeda, Y. Nakamura, K. Asakawa, and K. Inoue, Opt. Express **12,** 1090 (2004).
6. M. Gnan, I. Ntakis, P. Pottier, R. M. De la Rue, and P. Bassi, J. Opt. Networking **6,** 90 (2007).
7. M. Notomi, Phys. Rev. Lett. **87,** 253902 (2001).
8. S. McNab, N. Moll, and Y. Vlasov, Opt. Express **11,** 2927 (2003).
9. S. Olivier, Opt. Express **11,** 1490 (2003).
10. L. Cao, Y. Huang, X. Mao, F. Li, W. Zhang, and J. Peng, Chin. Phys. Lett. **25,** 2101 (2008).
11. X. Mao, Chin. Phys. Lett. **24,** 454 (2007).